A Model Order-Free Method for Stable States Extraction in Dynamic Functional Connectivity

Songke Fang[1], Vince D. Calhoun [2], Godfrey Pearlson[3], Peter Kochunov[4], Theo G.M. van Erp[5] and Yuhui Du[1*]

[1] School of Computer and Information Technology, Shanxi University, Taiyuan, China
[2] Tri-Institutional Center for Translational Research in Neuroimaging and Data Science, Georgia State University, Georgia Institute of Technology, Emory University, Atlanta, GA, USA
[3] Departments of Psychiatry and Neurobiology, Yale University, New Haven, CT, USA
[4] Maryland Psychiatric Research Center and Department of Psychiatry, University of Maryland, School of Medicine, Baltimore, MD, USA
[5] Department of Psychiatry and Human Behavior, School of Medicine, University of California, Irvine, CA, USA
duyuhui@sxu.edu.cn

Abstract. Dynamic functional connectivity (dFC) analysis has revealed that functional connectivity fluctuates over short timescales, reflecting the intrinsic transitions of brain among multiple states. However, dFC data typically exhibit the characteristics of high dimensionality and noise, making it difficult to extract stable and accurate states. Furthermore, accurately identifying model order (i.e., number of states) is challenging due to lack of prior knowledge. To address the above issues, we propose a model order-free method for extracting stable states. Our method can simultaneously capture multi-scale state information and improve the stability of the state. Furthermore, our method estimates the number of states adaptively based on data-driven methods. Based on synthetic data, we evaluated the effectiveness of our method. The results showed that, compared to traditional methods, our method not only accurately estimated the number of states but also extracted states with greater robustness and precision. Additionally, we evaluated the effectiveness and stability of the method using fMRI data from 602 healthy controls and 519 schizophrenia patients. Results demonstrated that our method exhibited significant consistency among the states extracted by multiple runs. Moreover, we identified reliable biomarkers for schizophrenia. In conclusion, we propose a novel state extraction method that does not rely on predefined state numbers, while accurately and stably identifying states.

Keywords: Resting-state functional magnetic resonance imaging, Dynamic functional connectivity, Clustering.

1 Introduction

Resting-state functional magnetic resonance imaging (rs-fMRI) provides a way to quantify the functional interaction of the human brain. Functional connectivity (FC) has been extensively used to study how brain regions efficiently collaborate. Recent

evidence suggests that FC exhibits rapid, non-stationary fluctuations, indicating the intrinsic transitions of brain among multiple metastable states [1]. These dynamic changes in FC are critical for understanding the neural mechanisms underlying mental disorders and for identifying potential biomarkers [2].

To characterize the dynamic changes in the brain, the sliding window method is widely used in the study of dynamic functional connectivity (dFC). Since FC patterns across different subjects do not have a direct correspondence, researchers typically use clustering to unveil the underlying connectivity states [3]. However, dFC data typically exhibit the characteristics of high dimensionality and high noise, so it is difficult to extract stable and accurate states by traditional methods. Furthermore, in the absence of prior knowledge, determining the model orders (i.e., number of states) that describe the relationships between dFC patterns is also a challenge. A lower model order often struggles to capture the temporal changes in the brain, while a higher model order is more susceptible to noise. Although some studies attempt to pre-determine model order using the elbow criterion, the complex structure of dFC data lacks a clear elbow or presents multiple elbows [4]. Additionally, traditional methods typically fix single model order for state extraction, but the states obtained under different model orders may capture distinct underlying information.

To address the above issues, our study proposes a model order-free method for the extraction of stable states across multiple model orders. To the best of our knowledge, this is the first attempt to extract stable states across different model orders. The main contributions of this paper are summarized as follows:

1. A model order-free state extraction method is introduced which not only retains the multi-scale state information but also significantly improves the stability of the states.
2. A novel inter-cluster similarity graph is derived, which maps the dFC data into a multi-scale similarity graph composed of stable state clusters, making the clustering structure more obvious.
3. Experiments on synthetic datasets with varying characteristics demonstrate that the proposed method effectively estimates the number of states and outperforms existing methods in state extraction accuracy.
4. Experiments on fMRI dataset with 602 healthy controls (HCs) and 519 schizophrenia patients (SZs) demonstrate that proposed method can extract stable states. Furthermore, reliable biomarkers for schizophrenia are identified in the subcortical network.

2 Methods

The pipeline of the method proposed in this paper is shown in Fig. 1. In order to preserve the multi-scale state information and improve state stability, we propose an index to measure the stability of the basic states in order to achieve the extraction of stable states across scales. Subsequently, we introduce a novel inter-cluster similarity graph, which reflects the multi-scale correlation of stable states, making the clustering structure more obvious. For the obtained inter-cluster similarity graph, we merge

similar stable states into meta-states through community detection, and assign each window to the meta-state by voting.

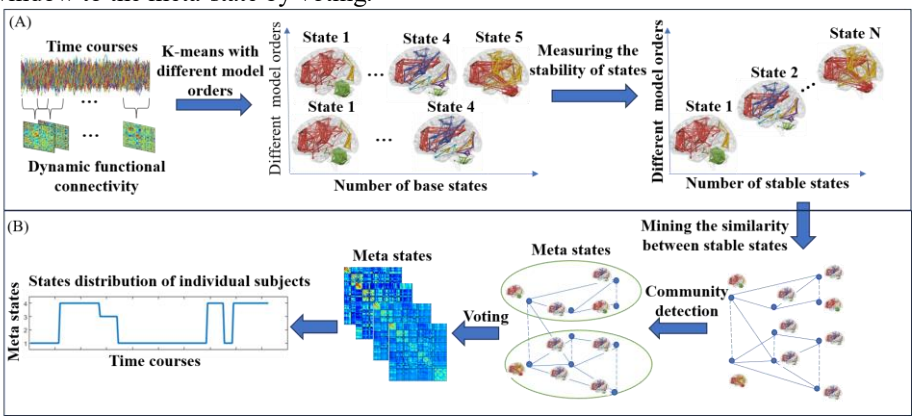

Fig. 1. The pipeline of the proposed method. (A) Identification of stable clusters across model orders (B) Measuring inter-cluster similarity between stable clusters to extract stable meta-states.

2.1 Identification of Stable States across Model Orders

In order to extract stable states at multiple model orders, we generate basic states under different model orders and evaluate the stability of the basic states (Fig. 1(A)). Specifically, let $X = \{x_i\}_{i=1}^{N}, x_i \in \mathbb{R}^d$ denote the dFC windows of all subjects, where x_i represents the i-th window, and d represents the upper triangular elements extract from each dFC window matrix. In the model orders range $[a, b]$, the K-means is executed m times independently with random initialization, yielding an ensemble of clustering solutions $\Pi = \{\pi_1, \cdots, \pi_m\}$. Each $\pi_k \in \Pi$ consists of a set of base clusters (i.e., states) $\pi_k = \left\{c_k^1, \cdots, c_k^{|\pi_k|}\right\}$, with each window x_i assigned a unique cluster label in $\pi_k(x_i)$.

Since different initializations and model orders can lead to significantly varied clusters [5], therefore we extract a stable subset of base clusters. Let $BC = \left\{c_1^1, \cdots, c_1^{|\pi_1|}, \cdots, c_k^1, \cdots, c_k^{|\pi_k|}\right\}$ be the set of all base clusters. Given a subset $SC \subseteq BC$, any clusters of BC that meets the predefine stability threshold σ will be added to the SC set, as show below:

$$SC = \begin{cases} c_k^l \in SC, & if\ AS(c_k^l) > \sigma \\ c_k^l \notin SC, & otherwise \end{cases}, \quad k \in [1, m], l \in [1, |\pi_k|] \qquad (1)$$

where $AS(c_k^l)$ is the stability of the l-th cluster in the k-th clustering solution. We use the normalized mutual information (NMI) measure to calculate the stability of base clusters. For a given cluster c_k^l in the π_k, we transform π_k into $\pi_\alpha = \left\{c_k^l, \widehat{c_k^l}\right\}$ with two clusters c_k^l and $\widehat{c_k^l}$, where $\widehat{c_k^l}$ contains all windows that do not in c_k^l. Also, let $\pi_\beta = \left\{c_u^l, \widehat{c_u^l}\right\}$ be another partition π_u with two clusters c_u^l and $\widehat{c_u^l}$ where c_u^l contains all 'positive clusters', if more than half of its windows overlap with c_k^l. Accordingly, the stability of c_k^l in π_β can be considered as NMI(π_α, π_β) and calculate as shown $SC(c_k^l, \pi_\beta)$

= NMI(π_α, π_β) For each $c_k^l \in BC$, there is a stability metric in partition π_k, thus the average stability is calculated as follows:

$$AS(c_k^l) = \frac{1}{m}\sum_{k=1}^{m} SC(c_k^l, \pi_k) \tag{2}$$

where m represents the number of partitions. The resulting stable states capture multi-scale dynamic information, serving as the basis for propagating inter-cluster similarities.

2.2 Propagation of Inter-cluster Similarity between Stable Clusters to Extract Stable Meta-States

As shown in Fig. 1(B), we propagate inter-cluster similarities through random walk to extract stable meta-states. We first construct an initial similarity graph $\mathrm{G} = \langle V, E, W \rangle$, where each node in V represents a stable cluster and the edge weight W between two stable clusters C_i, C_j is computed using the Jaccard coefficient $\omega_{ij} = \mathrm{Jaccard}(C_i, C_j)$. In order to integrate multi-scale information to construct inter-cluster similarity, we refine the initial graph using a multi-scale random walk [6]. Specifically, the transition probability matrix $P = \{p_{ij}\}$ is calculated as follows:

$$p_{ij} = \begin{cases} \frac{\omega_{ij}}{\sum_{\mu=1,\mu\neq i}^{S} \omega_{i\mu}}, & if\ i \neq j \\ 0, & if\ i = j \end{cases} \tag{3}$$

where, p_{ij} is the probability that a random walker transits from nodes C_i to C_j in one step. Base on the one-step transition probability matrix, the transition probability matrix $P^{(t)}$ for a random walk of t steps can be obtained, that is:

$$P^{(t)} = \begin{cases} P, & if\ t = 1 \\ P^{(t-1)} * P, & if\ t > 1 \end{cases} \tag{4}$$

in $P^{(t)}$, $p_{i:}^t$ denote the probability distribution of stable cluster C_i transitioning to every other stable cluster after t steps of the random walk. Different step lengths can reflect graph structural information at different scales [7], so we refine inter-cluster similarity via random walks with varying scales, where the aggregated transition probability from node C_i and reaching every other node in one to t steps is represented as: $\mathrm{PT}_{i:}^{(1:t)} = \sum_{u=1}^{t} p_{i:}^u$. We then compute similarity measure between nodes C_i and C_j:

$$z_{ij} = \frac{<\mathrm{PT}_{i:}^{(1:t)},\ \mathrm{PT}_{j:}^{(1:t)}>}{\sqrt{<\mathrm{PT}_{i:}^{(1:t)},\ \mathrm{PT}_{i:}^{(1:t)}> * <\mathrm{PT}_{j:}^{(1:t)},\ \mathrm{PT}_{j:}^{(1:t)}>}},\ z_{ij} \in [0,1] \tag{5}$$

z_{ij} is used as the weight in a new multi-scale weighted graph $\widetilde{\mathrm{G}} = \{\widetilde{\mathrm{V}}, \widetilde{\mathrm{E}}, \widetilde{\mathrm{W}}\}$, where $\widetilde{\mathrm{W}} = z_{ij}$ effectively captures the potential relationships among stable clusters at multiple scales. Here, the constructed multi-scale weighted graph adequately measures the potential relationships between stable clusters.

To obtain reliable meta-states, we apply the Louvain algorithm to perform community detection on $\widetilde{\mathrm{G}}$, selecting the community structure that maximizes modularity as the meta-states: $\mathrm{MC} = \{\mathrm{MC}_1, \mathrm{MC}_2, \cdots, \mathrm{MC}_K\}$, where K is the number of meta-states. Windows are assigned to meta-states via voting [8]. For a given window x_i and meta-state MC_j, the voting score is defined as:

$$\mathrm{Score}(x_i, \mathrm{MC}_j) = \frac{1}{|\mathrm{MC}_j|}\sum_{C_h \in \mathrm{MC}_j} \delta(x_i \in C_h) \tag{6}$$

where $\delta(x_i \in C_h)$ equals 1 if x_i is contained in C_h and 0 otherwise.

$$\text{MetaCls}(x_i) = \text{argmax}_{MC_j \in MC} \text{Score}(x_i, \text{MC}_j) \quad (7)$$

Here, each window x_i can be assigned to the meta-states with the highest vote count. Finally, the group-level functional connectivity state is formed by calculating the centroid of all windows in each meta-stable.

3 Materials and Experiments

3.1 Synthetic Datasets

For the synthetic datasets, we used the SimTB [9] to generate time courses (TCs), followed by a sliding window to estimate the dFC [10]. We generated synthetic data with different parameter combinations (Table 1) to evaluate the performance of different methods under different noise levels, different numbers of nodes and different numbers of states. Low and high noise were generated by varying the probability and amplitude of unique events in the underlying neural TCs, and the amplitude of Gaussian noise added to the TCs. We generated 50 subjects for each synthetic dataset, with each subject comprising 270 time points. For each subject, dFC was estimated using a tapered window, followed by extraction of upper triangular elements from each dFC matrix as feature vectors which were then concatenated along the window direction.

Table 1. Descriptions of synthetic datasets.

Datasets	Noise levels	Number of nodes	Number of states
Synthetic dataset 1	Low noise	25	5
Synthetic dataset 2	High noise	25	3
Synthetic dataset 3	High noise	25	5
Synthetic dataset 4	High noise	50	5

3.2 fMRI datasets and Preprocessing

The fMRI data included 602 HCs and 519 SZs from four datasets: BSNIP [11], COBRE [12], FBIRN [13], and MPRC [14]. The details of data preprocessing were described in [15]. Subsequently, for each subject, we extracted TCs from 116 regions of interest using the AAL template. These TCs were used to compute dFC via a tapered sliding window (window length = 20 TR, step size = 1 TR). Based on previous literature [16, 17], we mapped AAL to nine brain networks. For each window, we extracted upper triangular elements as an FC feature vector ($d = 6670$) and concatenated along the window direction. For the dFC data after concatenation, we used PCA to reduce the feature vector dimensionality to 1000 for improved computational efficiency.

3.3 Experiment and Evaluation

In the synthetic datasets experiments, based on multiple synthetic datasets we compared the relevant methods, including K-means with correlation, L1 and L2 distance, hierarchical clustering, and spectral clustering. We directly assigned the true number of clusters to the traditional methods. We did not include deep learning-based dFC methods in our comparison, because these methods primarily focus on obtaining better features, whereas our method aimed to extract states based on predefined features. For our method, we set the clustering model order to [2, 15], and employed the

K-means to generate 40 clustering solutions. Then, we extracted the stable clusters with stability exceeding the maximum value of 0.7 from among them. Based on previous literature [6], we set the step size of the random walk $t = 10$. We first assessed the ability of the proposed method to automatically infer the number of states from the synthetic datasets. To compare the performance of different methods in extracting states, we adopted Normalized Mutual Information (NMI) to assess the accuracy rate of the extracted labels.

In the fMRI experiments, our method employed the same clustering parameter settings as those used for the synthetic data. To further verify the effectiveness and interpretability of the method proposed in this paper in estimating the number of states, we applied the commonly used elbow criterion and our method respectively on the fMRI data to estimate the number of states. Subsequently, we repeated the method five times to evaluate the stability of the states. We employed the Hungarian algorithm [18] to align the estimated results from subsequent runs with those of the initial run. In addition, based on the subject-specific states corresponding to the same group-level state, we evaluated differences in connectivity strength between HCs and SZs using a two-tailed two-sample t-test.

4 Results

4.1 Results on Synthetic Datasets

Table 2 presents the average NMI scores (20 runs) by different methods. The results show that our method outperforms the comparison methods in terms of NMI on all synthetic datasets, indicating the proposed method can extract the states more accurately. Furthermore, the low standard deviation across multiple runs highlights the robustness and stability of our method. Regarding the estimation of the number of states, as shown in Table 2, for different synthetic datasets, we obtain stable and accurate number of states (20 runs), demonstrating the effectiveness of our method in capturing the underlying states.

Table 2. NMI (mean ± std) and states number (mean ± std) were derived from different methods based on different synthetic datasets. All the results were the average of 20 runs. Method 1: K-means with correlation distance; Method 2: K-means with L1 distance; Method 3: K-means with L2 distance; Method 4: hierarchical clustering; Method 5: spectral clustering.

Synthetic datasets	Method 1	Method 2	Method 3	Method 4	Method 5	Our method	
	NMI	NMI	NMI	NMI	NMI	States number	NMI
Synthetic datasets 1	0.79 ± 0.06	0.40 ± 0.04	0.50 ± 0.03	0.53 ± 0.00	0.05 ± 0.00	5.00 ± 0.00	**0.82 ± 0.00**
Synthetic datasets 2	0.62 ± 0.00	0.18 ± 0.05	0.50 ± 0.10	0.47 ± 0.00	0.01 ± 0.01	3.00 ± 0.00	**0.65 ± 0.01**
Synthetic datasets 3	0.57 ± 0.04	0.17 ± 0.04	0.50 ± 0.10	0.32 ± 0.00	0.03 ± 0.00	4.95 ± 0.22	**0.59 ± 0.01**

Synthetic datasets 4	0.74 ± 0.07	0.11 ± 0.10	0.40 ± 0.09	0.40 ± 0.00	0.05 ± 0.01	4.95 ± 0.22	**0.78 ± 0.01**

4.2 Results on fMRI Datasets

The Effectiveness of Estimating the Number of States. As shown in Fig. 2(A), no obvious elbow appears on the fMRI data, indicating that the method relying only on global clustering features is insufficient to reliably capture the underlying states in fMRI datasets. In contrast, Fig. 2(B) presents the t-SNE projection of the inter-cluster similarity matrix after community detection, where the obtained meta-clusters show obvious separability.

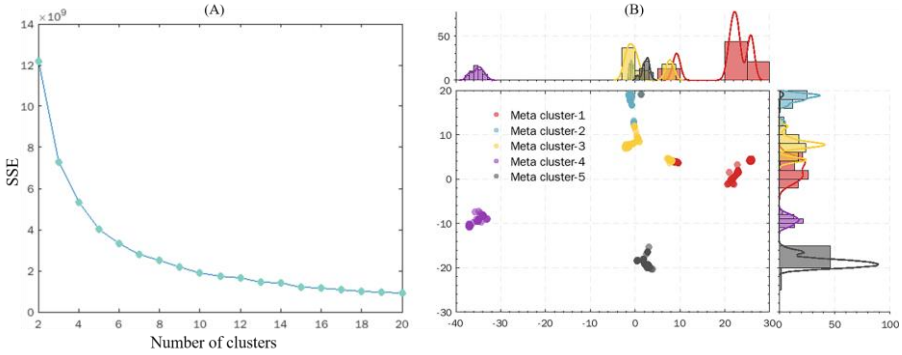

Fig. 2. State number estimation using (A) the method based on the elbow criterion and (B) the method proposed in this paper. SSE: sum of squared errors

The Stability of Extracted States. Fig. 3(A) shows that the correlations across states extracted in five independent runs are high (most typically over 0.85), reflecting the robustness of the proposed method. Additionally, we assess the stability of the extracted HC and SZ states across multiple runs (Fig. 3(B)). The results show that the correlation between different states typically exceeds 0.9, indicating that the states extracted by our method are highly reproducible.

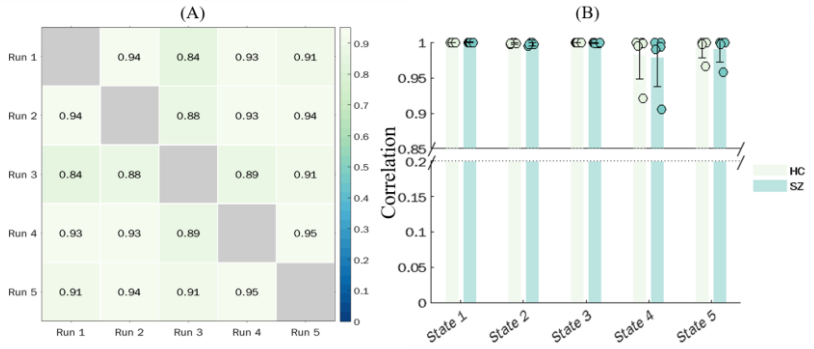

Fig. 3. Consistency evaluation across multiple runs on fMRI datasets. (A) Correlation of the state time courses across different runs of the method. (B) Correlation between HCs and SZs states from five runs of the method.

The Differences in Individual States Between HCs and SZs Groups. Fig. 4(A) shows the group-level states extracted by our method. The group differences among five identified connectivity states are shown in Fig. 4(B). In our results, each state shows significant group differences after two-sample t-tests ($p < 0.001$ with Bonferroni correction). The results reveal consistent and specific alterations in functional connectivity patterns of SZs across various states. Specifically, in almost all states, HCs exhibit lower connectivity strength than SZs in connectivity between subcortical network (SCN) and default mode network, as well as between SCN and sensorimotor network. Conversely, HCs display higher connectivity strength than SZs in connectivity between SCN and cerebellum. In fact, the loops that link cerebellum with cortical cortex are considered to be anatomically connected through thalamus. Thus, altered cerebellar-thalamus connectivity appeared to play a crucial role in this distributed circuit in schizophrenia [19].

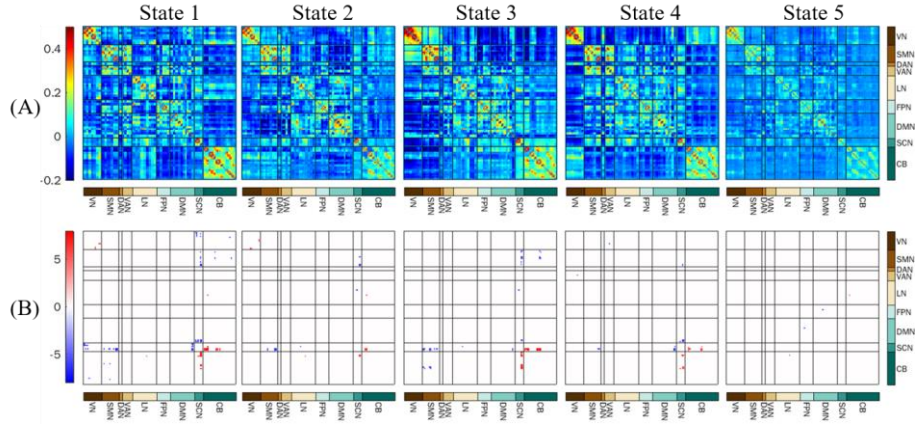

Fig. 4. Differences of states between HC and SZ groups. (A) Reliable group-level functional connectivity states. (B) The group differences between HCs and SZs in each state, tested by two-tailed two-sample t-tests ($p<0.001$ with Bonferroni correction).

5 Conclusion

This paper introduced a novel method for extracting stable states which was used to identify accurate and stable connectivity patterns without pre-determining the number of states. A key innovation lay in our ability to simultaneously retain multi-scale state information and significantly improve the stability of the states. A novel inter-cluster similarity graph was introduced that captured connections between stable states at different scales, making the clustering structure more distinct. Furthermore, our method estimated the number of states adaptively based on data-driven methods,

without requiring prior knowledge. The proposed method was applied to synthetic datasets and fMRI datasets, which verified its effectiveness and stability in extracting states and identified the functional connectivity of subcortical network related to schizophrenia as a key biomarker. Overall, the proposed method advances dFC analysis, providing a powerful and intuitive method for exploring brain function dynamics.

Acknowledgments. The work was supported by the National Natural Science Foundation of China (62076157 and 61703253, to Yuhui Du) and the National Institutes of Health(R01MH123610, to Vince D. Calhoun).

Disclosure of Interests. The authors have no competing interests to declare that are relevant to the content of this article.

References

1. Hancock, F. et al. (2025) Metastability demystified — the foundational past, the pragmatic present and the promising future. Nature Reviews Neuroscience 26 (2), 82-100.
2. Bolton, T.A.W. et al. (2020) Tapping into Multi-Faceted Human Behavior and Psychopathology Using fMRI Brain Dynamics. Trends in Neurosciences 43 (9), 667-680.
3. Allen, E.A. et al. (2014) Tracking Whole-Brain Connectivity Dynamics in the Resting State. Cerebral Cortex 24 (3), 663-676.
4. Vergara, V.M. et al. (2020) Determining the number of states in dynamic functional connectivity using cluster validity indexes. Journal of Neuroscience Methods 337, 108651.
5. Abbasi, S.-o. et al. (2019) Clustering ensemble selection considering quality and diversity. Artificial Intelligence Review 52 (2), 1311-1340.
6. Huang, D. et al. (2021) Enhanced Ensemble Clustering via Fast Propagation of Cluster-Wise Similarities. IEEE Transactions on Systems, Man, and Cybernetics: Systems 51 (1), 508-520.
7. Lai, D. et al. (2010) Enhanced modularity-based community detection by random walk network preprocessing. Physical Review E 81 (6), 066118.
8. Strehl, A. and Ghosh, J. (2003) Cluster ensembles --- a knowledge reuse framework for combining multiple partitions. 3 (null %J J. Mach. Learn. Res.), 583–617.
9. Erhardt, E. et al. (2012) SimTB, a simulation toolbox for fMRI data under a model of spatiotemporal separability. NeuroImage 59 (4), 4160-4167.
10. Spencer, A.P.C. and Goodfellow, M. (2022) Using deep clustering to improve fMRI dynamic functional connectivity analysis. NeuroImage 257, 119288.
11. Tamminga, C.A. et al. (2014) Bipolar and Schizophrenia Network for Intermediate Phenotypes: Outcomes Across the Psychosis Continuum. Schizophrenia Bulletin 40 (Suppl_2), S131-S137.
12. Aine, C.J. et al. (2017) Multimodal Neuroimaging in Schizophrenia: Description and Dissemination. Neuroinformatics 15 (4), 343-364.
13. Keator, D.B. et al. (2016) The Function Biomedical Informatics Research Network Data Repository. NeuroImage 124, 1074-1079.
14. Adhikari, B.M. et al. (2019) Functional network connectivity impairments and core cognitive deficits in schizophrenia. Human Brain Mapping 40 (16), 4593-4605.

15. Du, Y. et al. (2021) Evidence of shared and distinct functional and structural brain signatures in schizophrenia and autism spectrum disorder. Communications Biology 4, 1073.
16. YBT, T. et al. (2011) The organization of the human cerebral cortex estimated by intrinsic functional connectivity. Journal of Neurophysiology 106 (3), 1125-1165.
17. Long, Z. et al. (2023) Extended nonnegative matrix factorization for dynamic functional connectivity analysis of fMRI data. Cognitive Neurodynamics.
18. Munkres, J. (1957) Algorithms for the Assignment and Transportation Problems. Journal of the Society for Industrial and Applied Mathematics 5 (1), 32-38.
19. He, H. et al. (2019) Reduction in gray matter of cerebellum in schizophrenia and its influence on static and dynamic connectivity. Human Brain Mapping 40 (2), 517-528.